
Fighting Copycat Agents in Behavioral Cloning from Observation Histories

Chuan Wen^{*1}, Jierui Lin^{*2}, Trevor Darrell², Dinesh Jayaraman³, Yang Gao^{†124}

¹Institute for Interdisciplinary Information Sciences, Tsinghua University

²UC Berkeley, ³University of Pennsylvania, ⁴Shanghai Qi Zhi Institute

Abstract

Imitation learning trains policies to map from input observations to the actions that an expert would choose. In this setting, distribution shift frequently exacerbates the effect of misattributing expert actions to nuisance correlates among the observed variables. We observe that a common instance of this causal confusion occurs in partially observed settings when expert actions are strongly correlated over time: the imitator learns to cheat by predicting the expert’s *previous* action, rather than the next action. To combat this “copycat problem”, we propose an adversarial approach to learn a feature representation that removes excess information about the previous expert action nuisance correlate, while retaining the information necessary to predict the next action. In our experiments, our approach improves performance significantly across a variety of partially observed imitation learning tasks.

1 Introduction

Imitation learning is a simple, yet powerful paradigm for learning complex behaviors from expert demonstrations, with many successful applications ranging from autonomous driving to natural language generation [35, 40, 26, 28, 8, 16, 52]. The key idea underlying these successes is straightforward: given a training dataset of demonstrations by an expert, an agent’s action policy π can be trained by mapping demonstration states s_t to expert actions a_t .

Partially observed settings pose a problem for this approach: rather than the full state s_t , only observations o_t are available to the agent. As an example, for an autonomous car driving agent with a forward-facing camera, a single frame observation o_t from the camera omits much of the relevant state information for driving, such as the velocities of vehicles in front of the car, and the presence or absence of vehicles by its side. A policy trained to map o_t to actions a_t would thus be severely limited in such settings [13, 5, 19], especially in imitation learning. However, this limitation may in principle be alleviated by a simple fix: rather than training a policy $\pi(a_t|o_t)$, one could train a policy $\pi(a_t|\tilde{o}_t = [o_t, o_{t-1}, o_{t-2}, \dots])$, accessing past observations to fill in missing state information from the current observation.

In practice, several prior works have reported that imitation from observation histories sometimes performs *worse* than imitation from a single frame alone [51, 26, 6]. To illustrate why this happens, consider the sequence of actions in an expert demonstration when it starts to drive in response to a red traffic light turning green (Figure 1). Assuming an action space with only two actions,

*Equal contribution.

†Work done while at UC Berkeley.

cwen20@mails.tsinghua.edu.cn, jerrylin0928@berkeley.edu,

trevor@eecs.berkeley.edu, dineshj@seas.upenn.edu, gaoyangiiis@tsinghua.edu.cn

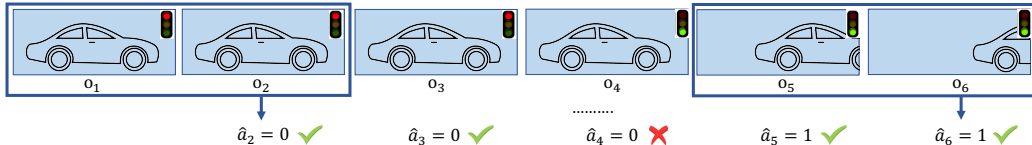


Figure 1: This figure demonstrates the “copycat” problem in an autonomous driving scenario. The top part of the figure shows a sequence of observations, where the vehicle waits at the red light and start to drive when the light turns green. The policy takes a sliding window of observations as input. At the bottom of the figure, we show that a “copycat” policy which simply replays its previous action will predict all but one actions correctly.

brake ($a = 0$), and throttle ($a = 1$), the sequence of expert actions over time would look like $[a_0 = 0, a_1 = 0, \dots, a_\tau = 0, a_{\tau+1} = 1, \dots, a_T = 1]$.

Which imitation policies would be effective at predicting the expert action on data from such demonstrations? Consider a “copycat” action policy that simply copies the previous expert action and prescribes repeating it as the next action. On these demonstrations, this policy would produce the correct action at all but one time instant, when the expert switches from braking to throttling. Our imitation learner $\pi(a_t|\tilde{o}_t)$ could easily express this copycat policy: it could recover the previous expert action a_{t-1} from the last two frames, o_t and o_{t-1} . The imitation training objective would encourage this, since this policy would produce low error on training and held-out demonstrations. However, when testing for actual driving performance, it would be useless — it would simply never switch to the throttle action.

We hypothesize that this copycat problem arises in imitation policies accessing past observations when two conditions are met: (i) expert actions over time are strongly correlated, and (ii) past expert actions are easily recovered from the observation history. As our first contribution, we empirically validate this hypothesis. We find that the temporal correlation among expert actions leads to even higher temporal correlation among learned policy actions. Further, the higher this temporal correlation, the worse the performance of the imitation learner (Section 4).

Then, we propose a novel imitation learning objective with an adversarial learning method that ensures that the imitation policy ignores the known nuisance correlate — the previous action a_{t-1} . Our implicit approach is scalable and robust, avoiding the need to learn disentangled representations [7], or learn a mixture of exponentially many graph conditioned policies [12] in previously proposed approaches tackling related problems. Our method only needs an offline expert demonstration dataset, unlike methods like DAGGER [39] and CCIL [12] which resolve the causal confusion through online expert queries, or GAIL [21] which needs online environment interaction. Inspired by robotics applications, we demonstrate our approach in six simulated continuous robotic control settings.

2 Related Work

Imitation Learning. Imitation learning [30, 2], first proposed by Widrow and Smith in 1964 [53], is a powerful learning paradigm that enables the learning of complex behaviors from demonstrations. We focus on the widely used behavioral cloning paradigm [35, 40, 26, 28, 8, 16], which suffers from a well-known problem: small errors in the learned policy compound over time, leading quickly to states outside the training demonstration distribution, where performance deteriorates. One solution is to assume access to a queryable expert who prescribes actions in the new states encountered by the policy, as in the widely-used DAGGER algorithm [39] and others [46, 25, 47]. Another well-studied alternative is to refine the policy through environment interaction [21, 9].

de Haan et al. [12] explicitly connected distributional shift problems in imitation settings to nuisance correlations between input variables and expert actions, identifying the “causal confusion” problem. We isolate this causal confusion problem in its most frequently occurring form, the copycat problem motivated in Sec 1, encountered by ML practitioners within imitation learning [26, 6, 11, 51] and elsewhere, as “feedback loops” [42, 4]. We demonstrate a scalable solution to the copycat problem.

Causal Discovery. While models produced by standard machine learning approaches may rely on nuisance correlates because they assume independent identically distributed samples at training and test time, *causal models* [33, 22, 34] instead uncover relationships that hold even under distributional shift. This connection between causality and distributional robustness has been studied in [20, 27, 10].

Existing causal discovery approaches, such as the widely used PC algorithm [44] as well as more recent techniques [7, 32, 18], operate over predefined, disentangled variables. However, in domains like vision or language, these underlying variables are unknown and must themselves be inferred from raw, high-dimensional observations, making causal discovery hard.

Most closely related to us, in the imitation learning setting, de Haan et al. [12] train a mixture of models on top of learned disentangled features in simple problem settings, exploiting environmental interactions afterwards to find the correct causal model. We take a different approach, sidestepping the difficulties of causal graph learning by injecting domain knowledge [29] to avoid nuisance correlates. Our approach is able to learn policies purely from demonstration data, requiring no environmental interaction afterwards. We compare against de Haan et al. [12] in more detail in later sections.

Adversarial Learning. “Adversarial” learning approaches, set up to resemble two agents competing against each other, have recently had great success in many application domains, such as image generation [17, 36, 23], and domain adaptation [50, 49, 14]. Our approach extends these adversarial losses to the imitation learning setting, setting up a nuisance correlate predictor as an adversary to the imitation policy.

3 Background and Problem Setup

Notation. We study behavioral cloning (BC) in a partially observed Markov decision process (POMDP). The POMDP states s_t transition as a function of agent actions a_t at time t , producing rewards r_t that specify the agent’s task within the environment. The agent does not have access to either the states s_t , or the rewards r_t . In lieu of states s_t , it has access to observations $o_t = f(s_t)$, where f is an unknown many-to-one function. In lieu of rewards r_t , the agent is provided with an expert’s demonstrations of desirable behavior through N_d expert demonstration trajectories $\{\mathcal{T}_i^e\}_{i=1}^{N_d}$. BC trains a parametrized policy $\pi_\theta(a_t|\tilde{o}_t)$ that prescribes the next action, given the last H observations $\tilde{o}_t = [o_t, o_{t-1}, o_{t-2}, \dots, o_{t-H+1}]$. In what follows, we will sometimes refer to observation histories \tilde{o} simply as observations, for brevity.

BC Training Objective. The final goal is to maximize the expected cumulative reward $R(\theta) = \mathbb{E}[\sum_t r_t]$ from executing π_θ in the environment. At training time, BC maximizes a different objective: the log-likelihood $L(\theta)$ of a dataset $\{(\tilde{o}_i, a_i^e)\}_{i=1}^N$ of N observation-action pairs drawn from the demonstrations, $\theta^* = \arg \max_\theta \sum_{i=1}^N \log \pi_\theta(a_i^e|\tilde{o}_i)$.

Distributional Shift. When the trained policy π_{θ^*} is executed in the environment, even minor deviations from the expert’s policy get compounded over time [39]. As a result, π_{θ^*} soon encounters observations \tilde{o}_t outside the training distribution, where its performance suffers. This distributional shift issue lies at the very core of the “copycat” problem studied in this paper.

4 The Copycat Problem

To introduce the copycat problem, we start by asking: what is the optimal value of H , the size of the observation history window, in the above setup? Conventional wisdom holds [30] that larger H would benefit the agent by providing more of the information contained in the state s_t . The only argument against large H would be that it might necessitate larger model capacity required to represent π_θ , risking overfitting to a finite demonstration dataset.

Yet, many prior works have reported [51, 26, 6, 11] that $H = 1$ is optimal. In other words, the *most poorly* observed setting, with $\tilde{o}_t = o_t$, yields the best results. Even more intriguingly, with $H > 1$, the likelihood $L(\theta^*)$ of held-out expert demonstrations improves, which means that there is no overfitting; only the environment reward $R(\theta^*)$ decreases. de Haan et al. [12] recently identified this problem as “causal confusion”: BC policies misattribute expert actions to demonstration-specific nuisance correlates that no longer hold under the aforementioned distributional shift induced by policy execution.

We go one step further, pinning the nuisance correlate in a prominent class of causal confusion problems to the previous expert action a_{t-1}^e , which is often recoverable from observation histories, as in the car example in Sec 1. When expert actions are strongly correlated over time, the imitation learner has a suboptimal, but tantalizingly convenient shortcut [15]: merely learning to recover the

Table 1: MSE for next action prediction, conditioned on previous actions. The lower the error for a policy, the higher its tendency to generate actions that can be predicted from previous actions alone.

	Ant $\times 10^{-2}$	Hopper $\times 10^{-3}$	Humanoid $\times 10^{-1}$	Reacher $\times 10^{-5}$	Walker2d $\times 10^{-2}$	HalfCheetah $\times 10^{-2}$
expert	6.91 ± 0.21	8.60 ± 1.09	6.93 ± 0.32	1.46 ± 0.37	2.47 ± 0.07	9.81 ± 0.33
BC-OH	0.66 ± 0.04	1.07 ± 0.16	0.18 ± 0.01	0.32 ± 0.05	0.46 ± 0.02	2.97 ± 0.15

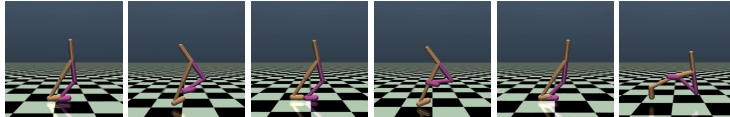


Figure 2: Frames of a copycat Walker2D agent falling (left to right): the right knee repeats previous actions at each time, failing to transition from an extended position to a bent position.

previous action very nearly maximizes the training objective $L(\theta)$. We call this the copycat problem, and posit that it accounts for many reported cases of causal confusion. Indeed, while de Haan et al. [12] propose to address the more general causal confusion problem, their experimental results are all in the copycat setting: they explicitly add a_{t-1} into o_t to induce causal confusion.

Empirical Evidence for the Copycat Problem. We now show qualitative and quantitative evidence demonstrating that the copycat problem occurs commonly in BC with partial observations. Motivated by robotic control, we use the six OpenAI Gym MuJoCo continuous control tasks. We set the history size $H = 2$ and train a neural network policy $\pi_\theta(a|\tilde{o}_t = [o_t, o_{t-1}])$ on expert demonstrations. We call this policy behavior cloning with observation histories (BC-OH). See Section 6 for more details.

To find a smoking gun for the copycat problem, we measure the predictability of the next action conditioned on the past actions, for a given policy. If the learner suffered from the copycat problem, this prediction would be easier on trajectories from the learned policy than on those from the expert policy. For each policy, we train a two-layer MLP to predict a_t given a_{t-1}, \dots, a_{t-k} as input. Here we use $k = 9$. Table 1 shows the mean-squared error (MSE) on held-out trajectories, on all six MuJoCo environments. In each case, the MSE is lower for the cloned BC-OH policy, than for the expert, pointing to the copycat problem.

Figure 2 shows six frames of a copycat BC-OH agent falling in Walker2d, where the agent fails to switch its right knee from an extended to a bent position to maintain balance. Other cases are even worse: for example, we observed copycat Half-Cheetah agents that did not ever start to move from a resting position.

It is clear that BC-OH policies exhibit an increased tendency to repeat actions (or more precisely, to generate actions that can be predicted from previous actions alone). To what extent does this affect their performance? For each environment, we now measure: (i) the action predictability ratio, the log-ratio of expert and BC-OH errors in Table 1, and (ii) the normalized reward, the average BC-OH reward divided by the average expert reward. Figure 3 shows a scatter plot of these metrics, showing that the action predictability ratio is inversely correlated with the normalized reward. In other words, a copycat imitation policy that copies past actions rather than responding to observations tends to perform worse.

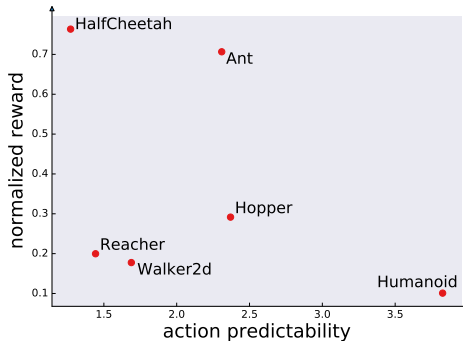


Figure 3: The action predictability metric (x-axis) versus the normalized reward (y-axis).

Figure 3 shows a scatter plot of these metrics, showing that the action predictability ratio is inversely correlated with the normalized reward. In other words, a copycat imitation policy that copies past actions rather than responding to observations tends to perform worse.

5 An Adversarial Solution to the Copycat Problem

We now propose an adversarial method to resolve the copycat problem. Our method builds on the standard behavioral cloning (BC) setup described in Sec 3. BC trains a policy $\pi_\theta(a_t|\tilde{o}_t)$ on expert demonstrations, to map from observation histories $\tilde{o}_t = [o_t, o_{t-1}, \dots, o_{t-H+1}]$ to expert actions.

For notational simplicity, we now restrict ourselves to deterministic policies, so that $a_t = \pi_\theta(\tilde{o}_t)$. For a policy represented by a multi-layer neural network, π_θ is easy to write as a composition of two learned functions, an encoder E and a decoder F : $a_t = \pi_\theta(\tilde{o}_t) = F(E(\tilde{o}_t))$. The output of the encoder network is a feature embedding $e_t = E(\tilde{o}_t)$.

Adversarial Nuisance Variable Prediction.

Fundamentally, the copycat problem arises from the fact that e_t contains information about the nuisance correlate a_{t-1} , and F learns to rely heavily on this information to predict a_t . This might suggest the following strategy: remove all information about a_{t-1} from the embedding e_t , so that F cannot rely on a_{t-1} at all. In other words, we would train the encoder E to maximize the conditional entropy $H(a_{t-1}|e_t)$, of the previous action, conditioned on the feature embedding. In practice, this means training an adversarial network D to predict a_{t-1} from e_t .

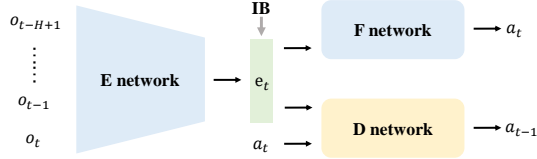


Figure 4: The network architecture. See Section 5 for explanations.

However, note that removing all information about a_{t-1} may be counterproductive: after all, the copycat problem arises only when a_t and a_{t-1} are highly correlated. Removing all information about a_{t-1} would make it very difficult to predict a_t . Put a different way, in order to predict a_t well, F requires some information about a_{t-1} to be retained in e_t .

Target-Conditioned Adversary (TCA). To account for this, we design a slightly different adversarial strategy. Rather than removing all information about a_{t-1} from e_t , we would like to remove only the information about a_{t-1} that is *not shared with* a_t . How might we set up an adversarial optimization process that removes this unshared information about a_{t-1} , while having no incentive to remove information that is actually useful for predicting the target variable a_t ? The solution is simple: the adversary D still tries to predict a_{t-1} from e_t , but with the target a_t as an additional conditioning input. The resulting optimization would train the encoder E to maximize the conditional entropy $H(a_{t-1}|e_t, a_t)$.

Intuitively, this means that the optimization process has no incentive to strip e_t of any information about a_{t-1} that is present in a_t — removing that information in e_t would not affect D ’s ability to predict a_{t-1} , since a_t contains the same information. Thus, no information about the target variable a_t is forcibly removed from the embedding. This means that the copycat solution of predicting the previous action is no longer a viable and convenient shortcut.

Information Bottleneck (IB). Further, we add an information bottleneck (IB) [1] between the encoder E and the decoder F to express the prior that any residual excess information in e_t should be ignored. Conceptually, our approach is built around identifying observation histories as likely to contain nuisance information. The target-conditioned Adversarial module only removes the information about a_{t-1} and the IB further removes other nuisance information. IB has been used in other works in similar ways Alemi et al. [1], Rakelly et al. [37], Pacelli and Majumdar [31]. Specifically, we modify E to predict the parameters μ_{e_t} and σ_{e_t} of an independent normal distribution, from which $e_t \sim p_E(e_t) = \mathcal{N}(\mu_{e_t}, \sigma_{e_t})$ is sampled. To apply an information bottleneck, we penalize the KL divergence between this distribution and the unit normal $\mathcal{N}(\mathbf{0}, \mathbf{I})$. Finally, D operates directly on μ_{e_t} , but F sees the “noisy” sample e_t . Intuitively, the IB implements a penalty for every bit of information that E transmits to F , encouraging it to transmit only the most essential information and ignore the nuisance correlate.

Finally, putting the target-conditioned adversary and the information bottleneck together, we have the following min-max optimization problem:

$$\min_{E, F} \max_D V(E, F, D) = \mathbb{E}_{e_t \sim p_E} \mathcal{L}(F(e_t), a_t) + \lambda KL(p_E(e_t) || \mathcal{N}(\mathbf{0}, \mathbf{I})) - \alpha \mathcal{L}(D(\mu_{e_t}, a_t), a_{t-1}),$$

where \mathcal{L} is an appropriate regression loss, such as the mean squared error.

Implementation Details. In our implementation, E , F , and D are all represented by neural networks. The overall network structure is depicted schematically in Fig 4. We train with stochastic gradient descent using the Adam optimizer. We use the reparametrization trick [24, 38] to evaluate the gradient through the expectation in the first term. We found that (1) different learning rates for E , F and D and (2) noise on the embedding e_t when training D , are helpful during optimization. In

our experiments, the encoder E is a 4-layer MLP, and the decoder F and the adversary D are each 2-layer MLPs. More details and pseudocode are in Appendix.

Connection to de Haan et al. [12]. As mentioned above, the phenomenon of causal confusion in imitation learning was identified in [12]. Their method, which we call CCIL, targets causal confusion in three steps: disentangled representation learning, policy learning conditioned on exponentially many causal graph structures, and online targeted interventions through environment interactions. They demonstrate results on simplified environments where a nuisance correlate is explicitly added into the state. In comparison, we focus on a more specific, but widely prevalent form of causal confusion (see Section 4), where the previous action is the nuisance correlate in imitation learning from observation histories — the copycat problem. This knowledge of the nuisance correlate drives our simpler, more robust, and more scalable approach, and allows us to perform experiments in more realistic settings: partially observed MDPs with history-aware imitation learners. Further, unlike CCIL, we demonstrate results on purely offline imitation: the imitation learner does not ever need to access the environment during training. We show experimental comparisons in Sec 6.

6 Experiments

In this section, we conduct experiments to evaluate our method against a variety of baselines. We also qualitatively study our method in order to better understand the newly introduced algorithm.

6.1 Baselines

We compare our method to the following baselines.

Behavioral cloning (BC-SO, BC-OH and RNN). **BC-SO** is naive behavioral cloning (Sec 3) with $H = 1$, which does not suffer from the copycat problem, since it cannot infer the previous action. However, BC-SO might suffer from lacking information to make an action decision. **BC-OH** is naive BC with $H > 1$. It allows the agent to access more of the state information necessary for optimal action selection, but it is prone to the copycat problem. We set k to 2 in our experiments. We train BC-OH agents both with stacked inputs to a feedforward policy, and with sequential inputs to an RNN policy.

Dropout-BC [6]. To combat causal confusion, Bansal et al. [6] add a neural net dropout layer [45], to the subset of inputs that might causally confuse the agent. Like our method, this method also assumes knowledge of the nuisance correlate. For this baseline, we add a dropout layer on the historical observations, i.e. o_{t-1}, o_{t-2}, \dots .

CCIL [12]. This is the method proposed in de Haan et al. [12], discussed in Sec 5. Note that our method assumes offline imitation, where we only have access to a pre-collected dataset, without any in-environment interactions. CCIL requires access to both. We set the number of environment interactions to 100.

DAGGER [39]. DAGGER is a widely used method to correct distributional shift in imitation learning. Similar to CCIL, DAGGER also requires environment interaction, with access to a queryable expert. We evaluate DAGGER at two values for the number of environment queries: 100 and 1000.

RL Expert [41]. We also compare against the RL expert, trained with TRPO [41], that was used to generate the expert data for imitation.

Aside from these baselines, we evaluate several ablations of our approach: Ours w/o Adversary, Ours w/o TCA, and Ours w/o IB, corresponding respectively to omitting the D network entirely, omitting only the target-conditioning in D , and omitting the information bottleneck.

6.2 Partially Observed Environments

Motivated by robotics applications, we evaluate our approach on all six MuJoCo [48] control environments from Open AI Gym: Ant, HalfCheetah, Hopper, Humanoid, Reacher and Walker2D. These tasks vary broadly in their state and action spaces, environmental dynamics, and reward structure. To evaluate the copycat problem, we make these environments partially observed in a natural way by setting the states to only include the joint positions and exclude other information i.e. velocity and external force. We train TRPO [41] agents without partial observability to generate

Table 2: Cumulative rewards per episode in partially observed (PO) environments. The top half of the table shows results in our offline imitation setting. The lower half shows methods that additionally interact with the environment, including accessing reinforcement learning rewards and queryable experts. CCIL cannot run on Ant and Humanoid because of their high-dimensional observations.

	PO-Ant	PO-Hopper	PO-Humanoid	PO-Reacher	PO-Walker2d	PO-HalfCheetah
BC-SO	1300 \pm 148	275 \pm 40	587 \pm 58	-79 \pm 5	363 \pm 86	-38 \pm 36
BC-OH	1750 \pm 146	293 \pm 83	565 \pm 80	-64 \pm 4	592 \pm 124	820 \pm 60
BC-OH (RNN)	-311 \pm 150	315 \pm 32	367 \pm 64	-75 \pm 5	190 \pm 14	830 \pm 398
Dropout-BC [6]	830 \pm 330	223 \pm 49	577 \pm 65	-80 \pm 7	283 \pm 194	406 \pm 165
Ours w/o Adversary	2030 \pm 88	473 \pm 129	638 \pm 101	-70 \pm 3	962 \pm 189	1260 \pm 68
Ours w/o TCA	1629 \pm 287	322 \pm 74	607 \pm 58	-55 \pm 3	1310 \pm 333	795 \pm 398
Ours w/o IB	1970 \pm 107	683 \pm 132	696 \pm 48	-57 \pm 4	929 \pm 266	1260 \pm 44
Ours	2150 \pm 34	1086 \pm 262	671 \pm 61	-54 \pm 4	1296 \pm 288	1250 \pm 42
RL Expert [41]	2348 \pm 5	1780 \pm 0	4963 \pm 47	-10 \pm 0	2428 \pm 2	1336 \pm 4
CCIL [12]	-	145 \pm 55	-	-68 \pm 6	474 \pm 134	714 \pm 132
DAGGER [39] (100 queries)	2090 \pm 34	978 \pm 216	688* \pm 47	-52 \pm 4	701 \pm 133	1080 \pm 86
DAGGER [39] (1k queries)	2240 \pm 14	1120 \pm 203	812* \pm 99	-15 \pm 2	2170 \pm 174	1270 \pm 22

* for Humanoid, we used 100k and 500k queries for DAGGER, instead of 100 and 1000.

expert demonstrations. See appendix for more details of those environments as well as the collection of the demonstration dataset.

6.3 Results and Analysis

Question 1. *Does our method improve performance over baseline approaches for behavioral cloning from observation histories?*

For each method, in each environment, we train five policies with varying random initializations, and report the mean and standard deviation of their cumulative rewards. Table 2 shows these results. Our full method performs best, or tied best across all six environments, among purely offline imitation methods. As expected, behavior cloning from single observation (BC-SO) performs poorly, due to partial observability. BC-OH, with observation histories, helps to varying extents in five out of six environments, but still performs much worse than the RL expert that generated the imitation trajectories. While the RNN hidden state can be thought of as implementing a natural information bottleneck, we find it performs similarly or worse than the feedforward BC-OH policies. Dropout-BC [6] was originally proposed and evaluated in a setting where the nuisance correlate corresponded to a single dimension in the input. This is not true in our settings, where the nuisance variable is a function of the high-dimensional past observations. It performs uniformly poorly across all tasks.

Among non-offline imitators, CCIL fails to achieve better rewards than our approach, even with additional environmental interaction and queryable experts. We believe that this is because it relies on learning a disentangled representation to handle high-dimensional observations, which it was unable to effectively do in our environments. DAGGER (100 queries) performs comparably with our purely offline method, and DAGGER (1000 queries) performs significantly better, approaching the performance of the RL expert in several settings. On Hopper and Humanoid, even the best imitators fall far short of the expert.

Question 2. *Which components of our method are most important to its performance?*

Comparing ablated variants of our approach in Table 2, the target-conditioned adversary (TCA) and the information bottleneck (IB) are both clearly important components. Our method without TCA performs the poorest out of our ablations in four out of six environments — recall that the unconditioned adversary could force the removal of too much important information from the learned embedding. Using only the information bottleneck without an adversary (Ours w/o Adversary) already yields significant improvements over BC-OH and Dropout-BC — we take this to mean that merely penalizing the description length of the learned representation encourages dropping nuisance information. Ours w/o IB, which only uses TCA, does nearly as well as our full method on most tasks, suggesting that the target-conditioned adversary is the most important component of our approach.

Question 3. *Does our policy truly rely less on the previous action a_{t-1} ?*

We train an MLP, in Hopper, to predict a_{t-1} from $[e_t, a_t]$ — recall that this is the function of the D -network in our algorithm. We use the test mean-squared error (MSE) score of this trained predictor

as a measure of the confounding excess information: the higher the score, the less excess information about a_{t-1} there is in e_t , and the better for avoiding copycat issues. For comparison, we compute the same MSE score for the BC-OH baseline. Finally, as an upper bound, we compute the MSE score for predicting a_{t-1} from a_t alone. Table 3 shows these scores. As expected, our approach w/o IB (i.e. TCA alone) removes nearly all of the confounding information from e_t , making a_{t-1} no easier to predict than from a_t alone. In other words, our approach successfully trains policies that do not overly rely on the previous action.

Table 3: The mean squared error for predicting the previous action a_{t-1} from various features.

setting	w/o IB	BC-OH	a_t
test MSE $\times 10^{-3}$	5.97 \pm 1.32	0.38 \pm 0.04	5.00 \pm 0.33

Question 4. *Does the TCA help to retain information that is useful for predicting the next action?*

Table 4 reports the BC testing error (next action prediction MSE) in Hopper for 3 methods: BC-OH, ours w/o IB (i.e. TCA only), and ours w/o IB and TCA (i.e. unconditional adversary loss only). While TCA cannot predict current action a_t as well as BC-OH, its performance is significantly better than the unconditional adversarial setting, indicating that the target-conditioning effectively preserves more information about the next action. Note that in terms of actual environmental reward, TCA performs the best, followed by the unconditioned adversary.

Table 4: The BC mean squared error (for predicting the next action a_t) on test data.

setting	w/o IB	w/o IB&TCA	BC-OH
test MSE $\times 10^{-3}$	9.48 \pm 1.89	14.62 \pm 1.41	0.89 \pm 0.12

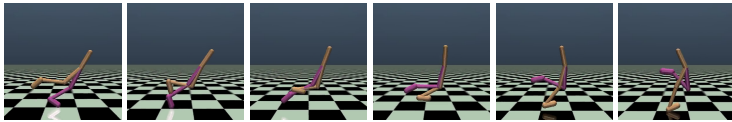


Figure 5: Our method solves the copycat problem, demonstrated in Walker2D. The agent no longer only moves one leg, but it starts to walk with both legs, in contrast to the BC-OH agent in Figure 2.

Question 5. *Does our policy repeat itself during test time?*

In Section 4, we show that the BC-OH baseline tends to repeat its own previous action during online rollouts. Here we use the same action predictability metric to test our method. Table 5 shows the result. We can see that our method reduces the correlation between consecutive actions. Figure 6 shows the impact on performance: our method reduces action predictability and increases reward in every environment, indicating that it successfully addresses the copycat problem.

Besides the action predictability score in Table 5, we now present an example of behavior where the copycat problem is visibly resolved. To compare with Figure 2, we visualize the Walker2D agent again in Figure 5. Our agent responds to its observations, rather than copying the previous action as BC-OH often did in Figure 2. The result is a doubling of the mean reward in this environment from BC-OH’s 592, to our 1296 (see Table 2).

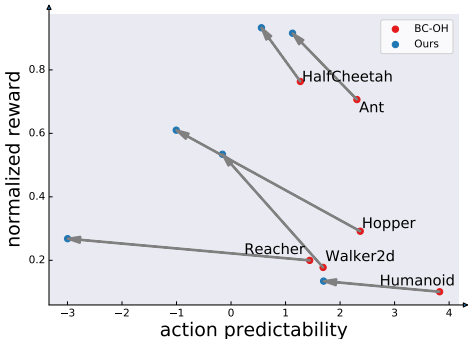


Figure 6: In all 6 environments, our method reduces action predictability, and improves the normalized reward, over the BC-OH baseline.

The result is a doubling of the mean reward in this environment from BC-OH’s 592, to our 1296 (see Table 2).

Table 5: Similar to Table 1, the predictability of the next action conditioned on past actions of our method and the BC-OH policy. Our method reduces the repetition of actions over time.

	Ant $\times 10^{-2}$	Hopper $\times 10^{-3}$	Humanoid $\times 10^{-1}$	Reacher $\times 10^{-5}$	Walker2d $\times 10^{-2}$	HalfCheetah $\times 10^{-2}$
BC-OH	0.66 \pm 0.04	1.07 \pm 0.16	0.18 \pm 0.01	0.32 \pm 0.05	0.46 \pm 0.02	2.97 \pm 0.15
Ours	2.20 \pm 0.06	2.26 \pm 0.12	1.33 \pm 0.02	2.99 \pm 0.36	3.07 \pm 0.08	5.40 \pm 0.20

7 Conclusion and Future Work

In this paper, we identify the copycat problem that commonly afflicts imitation policies learning from histories of observations. We systematically study this phenomenon by carefully designing a set of diagnostic experiments, which shows the existence of this problem in multiple environments. Finally, we propose a new adversarial mechanism to tackle this problem. We validate our approach through extensive comparisons with previous approaches on 6 standard continuous control benchmark tasks. Our method significantly alleviates the copycat problem for offline behavioral cloning from observation histories, and even outperforms some existing online behavioral cloning methods that have additional access to the environment. As for future work, while our method works pretty well in state-based environments, the improvement in image-based experiments is not significant yet. The causal confusion in image-based control is still an open question and we hope to address these more realistic scenarios in the future.

8 Broader Impact

In this paper, we introduce a systematic approach to combat the “copycat” problem in behavioral cloning with observation histories. Behavioral cloning can be applied to a wide range of applications, such as robotics, natural language, decision making, as well as economics. Our method is particularly useful for offline behavioral cloning with partially observed states.

Offline imitation is currently one of the most promising ways to achieve learned control in the world. Our method can improve the real world performance of behavior cloning agents, which could enable wider use of behavior cloning agents in practice. This could help to automate repetitive processes previously requiring human workers. While on the one hand, this has the ability to free up human time and creativity for more rewarding tasks, it also raises the concerning possibility of the loss of blue collar jobs. To mitigate the risks, it is important to promote policy and legislation to protect the interests of the workers who might be affected during the adoption of such technology.

9 Acknowledgements

We are grateful to Pim de Haan, Jianing Qian, and Sergey Levine for fruitful discussions and comments.

References

- [1] Alexander A Alemi, Ian Fischer, Joshua V Dillon, and Kevin Murphy. Deep variational information bottleneck. *arXiv preprint arXiv:1612.00410*, 2016.
- [2] Brenna D Argall, Sonia Chernova, Manuela Veloso, and Brett Browning. A survey of robot learning from demonstration. *Robotics and autonomous systems*, 57(5):469–483, 2009.
- [3] Martín Arjovsky and Léon Bottou. Towards principled methods for training generative adversarial networks. In *5th International Conference on Learning Representations, ICLR 2017, Toulon, France, April 24-26, 2017, Conference Track Proceedings*. OpenReview.net, 2017. URL https://openreview.net/forum?id=Hk4_qw5xe.
- [4] Drew Bagnell. Feedback in machine learning, 2016. URL <https://www.youtube.com/watch?v=XRSvz4UOp04>.

- [5] Bram Bakker. Reinforcement learning by backpropagation through an lstm model/critic. In *2007 IEEE International Symposium on Approximate Dynamic Programming and Reinforcement Learning*, pages 127–134. IEEE, 2007.
- [6] Mayank Bansal, Alex Krizhevsky, and Abhijit Ogale. Chauffeurnet: Learning to drive by imitating the best and synthesizing the worst. *arXiv preprint arXiv:1812.03079*, 2018.
- [7] Yoshua Bengio, Tristan Deleu, Nasim Rahaman, Nan Rosemary Ke, Sebastien Lachapelle, Olexa Bilaniuk, Anirudh Goyal, and Christopher Pal. A meta-transfer objective for learning to disentangle causal mechanisms. In *International Conference on Learning Representations*, 2020.
- [8] Mariusz Bojarski, Davide Del Testa, Daniel Dworakowski, Bernhard Firner, Beat Flepp, Prasoon Goyal, Lawrence D. Jackel, Mathew Monfort, Urs Muller, Jiakai Zhang, Xin Zhang, Jake Zhao, and Karol Zieba. End to end learning for self-driving cars. *CoRR*, abs/1604.07316, 2016.
- [9] Kianté Brantley, Wen Sun, and Mikael Henaff. Disagreement-Regularized Imitation Learning. *International Conference in Learning Representations*, pages 1–19, 2020.
- [10] Peter Bühlmann. Invariance, causality and robustness. *arXiv preprint arXiv:1812.08233*, 2018.
- [11] Felipe Codevilla, Eder Santana, Antonio M López, and Adrien Gaidon. Exploring the limitations of behavior cloning for autonomous driving. In *Proceedings of the IEEE International Conference on Computer Vision*, pages 9329–9338, 2019.
- [12] Pim de Haan, Dinesh Jayaraman, and Sergey Levine. Causal confusion in imitation learning. In *Advances in Neural Information Processing Systems*, pages 11693–11704, 2019.
- [13] Yan Duan, John Schulman, Xi Chen, Peter L Bartlett, Ilya Sutskever, and Pieter Abbeel. RI^2 : Fast reinforcement learning via slow reinforcement learning. *arXiv preprint arXiv:1611.02779*, 2016.
- [14] Yaroslav Ganin and Victor Lempitsky. Unsupervised domain adaptation by backpropagation. In *Proceedings of the 32nd International Conference on International Conference on Machine Learning - Volume 37, ICML'15*, page 1180–1189. JMLR.org, 2015.
- [15] Robert Geirhos, Jörn-Henrik Jacobsen, Claudio Michaelis, Richard Zemel, Wieland Brendel, Matthias Bethge, and Felix A Wichmann. Shortcut learning in deep neural networks. *arXiv preprint arXiv:2004.07780*, 2020.
- [16] Alessandro Giusti, Jérôme Guzzi, Dan C Cireşan, Fang-Lin He, Juan P Rodríguez, Flavio Fontana, Matthias Faessler, Christian Forster, Jürgen Schmidhuber, Gianni Di Caro, et al. A machine learning approach to visual perception of forest trails for mobile robots. *IEEE Robotics and Automation Letters*, 1(2):661–667, 2015.
- [17] Ian Goodfellow, Jean Pouget-Abadie, Mehdi Mirza, Bing Xu, David Warde-Farley, Sherjil Ozair, Aaron Courville, and Yoshua Bengio. Generative adversarial nets. In *Advances in neural information processing systems*, pages 2672–2680, 2014.
- [18] Anirudh Goyal, Alex Lamb, Shagun Sodhani, Jordan Hoffmann, Sergey Levine, Yoshua Bengio, and Bernhard Scholkopf. Recurrent independent mechanisms, 2020. URL <https://openreview.net/forum?id=BylaUTNtPS>.
- [19] Matthew Hausknecht and Peter Stone. Deep recurrent q-learning for partially observable mdps. *arXiv preprint arXiv:1507.06527*, 2015.
- [20] Christina Heinze-Deml and Nicolai Meinshausen. Conditional variance penalties and domain shift robustness. *arXiv preprint arXiv:1710.11469*, 2017.
- [21] Jonathan Ho and Stefano Ermon. Generative adversarial imitation learning. In D. D. Lee, M. Sugiyama, U. V. Luxburg, I. Guyon, and R. Garnett, editors, *Advances in Neural Information Processing Systems 29*, pages 4565–4573. Curran Associates, Inc., 2016.
- [22] Guido W Imbens and Donald B Rubin. *Causal inference in statistics, social, and biomedical sciences*. Cambridge University Press, 2015.

- [23] Tero Karras, Samuli Laine, and Timo Aila. A style-based generator architecture for generative adversarial networks. In *Proceedings of the IEEE Conference on Computer Vision and Pattern Recognition*, pages 4401–4410, 2019.
- [24] Diederik P Kingma and Max Welling. Auto-encoding variational bayes. *ICLR*, 2014.
- [25] Michael Laskey, Jonathan Lee, Roy Fox, Anca Dragan, and Ken Goldberg. Dart: Noise injection for robust imitation learning. In *Conference on Robot Learning*, pages 143–156, 2017.
- [26] Yann LeCun, Urs Muller, Jan Ben, Eric Cosatto, and Beat Flepp. Off-road obstacle avoidance through end-to-end learning. *Advances in Neural Information Processing Systems*, pages 739–746, 2005. ISSN 10495258.
- [27] Nicolai Meinshausen. Causality from a distributional robustness point of view. In *2018 IEEE Data Science Workshop (DSW)*, pages 6–10. IEEE, 2018.
- [28] Katharina Mülling, Jens Kober, Oliver Kroemer, and Jan Peters. Learning to select and generalize striking movements in robot table tennis. *The International Journal of Robotics Research*, 32(3):263–279, 2013.
- [29] Austin Nichols. Causal inference with observational data. *The Stata Journal*, 7(4):507–541, 2007.
- [30] T Osa, J Pajarinen, G Neumann, JA Bagnell, P Abbeel, and J Peters. An algorithmic perspective on imitation learning. *Foundations and Trends in Robotics*, 7(1-2):1–179, 2018.
- [31] Vincent Pacelli and Anirudha Majumdar. Learning task-driven control policies via information bottlenecks. *arXiv preprint arXiv:2002.01428*, 2020.
- [32] Giambattista Parascandolo, Niki Kilbertus, Mateo Rojas-Carulla, and Bernhard Schölkopf. Learning independent causal mechanisms. *35th International Conference on Machine Learning, ICML 2018*, 9(1):6432–6442, 2018.
- [33] Judea Pearl. *Causality: Models, reasoning, and inference, second edition*. Cambridge university press, 2011. ISBN 9780511803161. doi: 10.1017/CBO9780511803161.
- [34] Jonas Peters, Dominik Janzing, and Bernhard Schölkopf. *Elements of Causal Inference: Foundations and Learning Algorithms*. MIT Press, November 2017.
- [35] Dean A Pomerleau. Alvin: An autonomous land vehicle in a neural network. In *Advances in neural information processing systems*, pages 305–313, 1989.
- [36] Alec Radford, Luke Metz, and Soumith Chintala. Unsupervised representation learning with deep convolutional generative adversarial networks. In Yoshua Bengio and Yann LeCun, editors, *4th International Conference on Learning Representations, ICLR 2016, San Juan, Puerto Rico, May 2-4, 2016, Conference Track Proceedings*, 2016.
- [37] Kate Rakelly, Aurick Zhou, Chelsea Finn, Sergey Levine, and Deirdre Quillen. Efficient off-policy meta-reinforcement learning via probabilistic context variables. In *International conference on machine learning*, pages 5331–5340, 2019.
- [38] Danilo Jimenez Rezende, Shakir Mohamed, and Daan Wierstra. Stochastic backpropagation and approximate inference in deep generative models. In Eric P. Xing and Tony Jebara, editors, *Proceedings of the 31st International Conference on Machine Learning*, volume 32 of *Proceedings of Machine Learning Research*, pages 1278–1286, Beijing, China, 22–24 Jun 2014. PMLR.
- [39] Stéphane Ross, Geoffrey J. Gordon, and J. Andrew Bagnell. A reduction of imitation learning and structured prediction to no-regret online learning. *Journal of Machine Learning Research*, 15:627–635, 2011. ISSN 15324435.
- [40] Stefan Schaal. Is imitation learning the route to humanoid robots? *Trends in cognitive sciences*, 3(6):233–242, 1999.

- [41] John Schulman, Sergey Levine, Pieter Abbeel, Michael Jordan, and Philipp Moritz. Trust region policy optimization. In *International conference on machine learning*, pages 1889–1897, 2015.
- [42] David Sculley, Gary Holt, Daniel Golovin, Eugene Davydov, Todd Phillips, Dietmar Ebner, Vinay Chaudhary, and Michael Young. Machine learning: The high interest credit card of technical debt. In *SE4ML: Software Engineering for Machine Learning (NIPS 2014 Workshop)*. IEEE, 2014.
- [43] Casper Kaae Sønderby, Jose Caballero, Lucas Theis, Wenzhe Shi, and Ferenc Huszár. Amortised MAP inference for image super-resolution. *CoRR*, abs/1610.04490, 2016. URL <http://arxiv.org/abs/1610.04490>.
- [44] Peter Spirtes, Clark N Glymour, Richard Scheines, and David Heckerman. *Causation, prediction, and search*. MIT press, 2000.
- [45] Nitish Srivastava, Geoffrey Hinton, Alex Krizhevsky, Ilya Sutskever, and Ruslan Salakhutdinov. Dropout: a simple way to prevent neural networks from overfitting. *The journal of machine learning research*, 15(1):1929–1958, 2014.
- [46] Wen Sun, Arun Venkatraman, Geoffrey J. Gordon, Byron Boots, and J. Andrew Bagnell. Deeply AggreVaTeD: Differentiable imitation learning for sequential prediction. *34th International Conference on Machine Learning, ICML 2017*, 7:5090–5108, 2017.
- [47] Wen Sun, J. Andrew Bagnell, and Byron Boots. TRUNCATED HORIZON POLICY SEARCH: DEEP COMBINATION OF REINFORCEMENT AND IMITATION. In *International Conference on Learning Representations*, 2018.
- [48] Emanuel Todorov, Tom Erez, and Yuval Tassa. Mujoco: A physics engine for model-based control. In *2012 IEEE/RSJ International Conference on Intelligent Robots and Systems*, pages 5026–5033. IEEE, 2012.
- [49] Eric Tzeng, Judy Hoffman, Ning Zhang, Kate Saenko, and Trevor Darrell. Deep domain confusion: Maximizing for domain invariance. *arXiv preprint arXiv:1412.3474*, 2014.
- [50] Eric Tzeng, Judy Hoffman, Kate Saenko, and Trevor Darrell. Adversarial discriminative domain adaptation. In *Proceedings of the IEEE Conference on Computer Vision and Pattern Recognition*, pages 7167–7176, 2017.
- [51] Dequan Wang, Coline Devin, Qi-Zhi Cai, Philipp Krähenbühl, and Trevor Darrell. Monocular plan view networks for autonomous driving. In *IROS*, 2019.
- [52] Sean Welleck, Kianté Brantley, Hal Daumé III, and Kyunghyun Cho. Non-monotonic sequential text generation. *arXiv preprint arXiv:1902.02192*, 2019.
- [53] Bernard Widrow and Fred W Smith. *Pattern-recognizing control systems*, 1964.

10 Appendix

10.1 Capability of each method to resolve the copycat problem

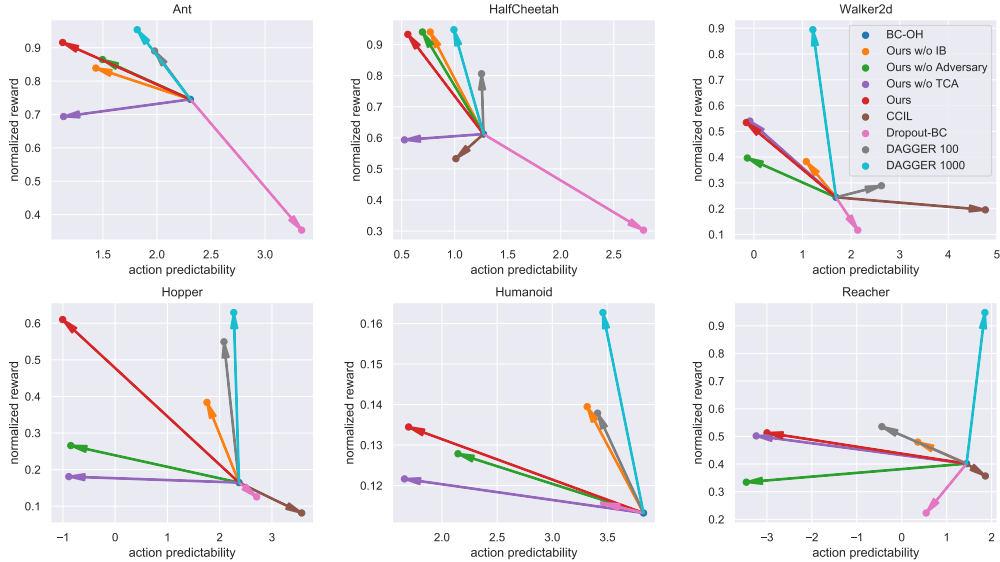


Figure 7: Normalized reward scores vs. action predictability. Arrows for each method start at BC-OH performance and end at the method’s performance.

In Figure 6, we showed that our method decreases action predictability, i.e. reduces the action repeat, and increases reward across all environments, over BC-OH baseline. Here, we present this result environment-wise, with additional arrows corresponding to baselines and ablations. The red arrow corresponds to our full method.

In nearly all environments, our approach yields the highest reward of all offline methods, and also achieves the lowest action predictability score. In three out of six environments, it approximately matches the performance of the even the best online imitation approach (DAGGER 1000, cyan).

10.2 Network architecture

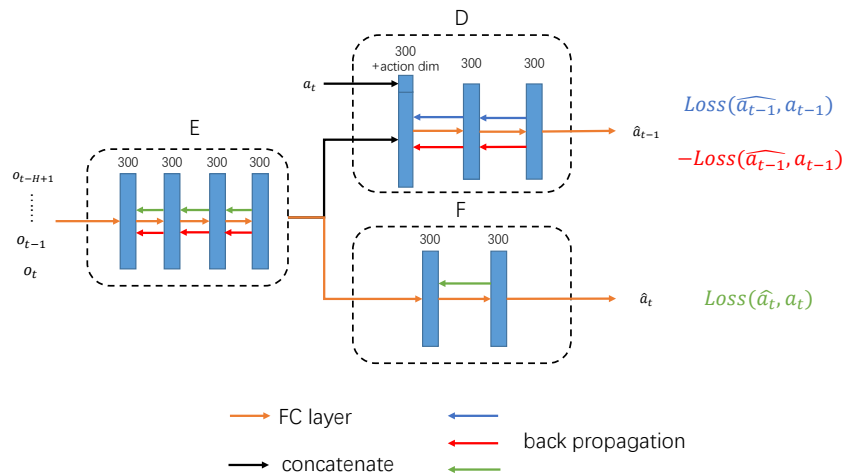


Figure 8: The architecture of target-conditioned adversarial model.

The network architecture of target-conditioned adversarial model is shown in Figure 8. We update the parameters in the neural network by the process shown in Algorithm 1.

Algorithm 1 Minibatch stochastic gradient descent training of the objective function.

Require: learning rate schedule of E and F , l_{EF} ; learning rate schedule of D , l_D ; embedding noise std σ ; batch size m ; number of frames in the imitation learning H

for number of training iterations **do**

- Sample minibatch of m examples $\{\mathcal{S}^{(1)}, \dots, \mathcal{S}^{(m)}\}$, where each $\mathcal{S}^{(i)} = \{(o_{t_i-H+1}, a_{t_i-H+1}), \dots, (o_{t_i}, a_{t_i})\}$ is a stack of H frames in the expert demonstration
- Update θ_E and θ_F by *descending* its gradient $\partial V/\partial\theta_E$ and $\partial V/\partial\theta_F$, with learning rate l_{EF} .
- Generate minibatch of m noise samples $\{\epsilon^{(1)}, \dots, \epsilon^{(m)}\}$, where $\epsilon^{(i)} \sim \mathcal{N}(0, \sigma^2 \mathbf{I})$.
- Add noise $\epsilon^{(i)}$ to $e^{(i)}$ in the computation graph, i.e. $e^{(i)} = e^{(i)} + \epsilon^{(i)}$ [3, 43]
- Update θ_D by *ascending* its gradient $\partial V/\partial\theta_D$, with learning rate l_D .

end for

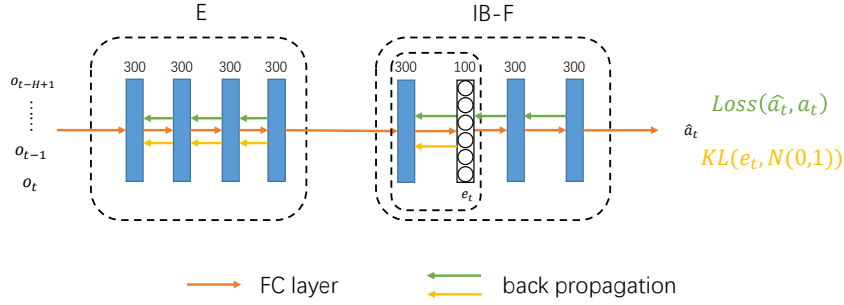


Figure 9: The architecture of information bottleneck model. The E network is pretrained by the target-conditioned adversarial model.

Our Information Bottleneck part, as shown in Figure 9, uses the encoder E pre-trained by the target-conditioned adversarial (TCA) model to initialize its encoder E . We add a information bottleneck module to the embedding generated by its encoder E and denote the combination of the bottleneck and the original F network as $IB-F$, which is optimized by the supervised loss $Loss(\hat{a}_t, a_t)$ and $KL(e_t, N(0,1))$.

10.3 Experiment Environments

Motivated by robotics applications, we compare our method with baselines and ablations on all six MuJoCo [48] control environments from Open AI Gym. Snapshots of these six environments are shown in Fig 10. The goal of Ant, Humanoid, Walker2d and HalfCheetah is to make the agent walk or run as fast as possible while Hopper’s objective is to make the agent hop forward as fast as possible and Reacher’s objective is to enable the robot reach a randomly located target.

10.4 Expert Data Collection

To collect expert demonstrations, we first train an expert with reinforcement learning, specifically TRPO [41]. This expert policy is executed in the environment to collect demonstrations. Since the six environments have very different observation dimensions, we collect 1k transitions for HalfCheetah, Reacher and Ant, 20k transitions for Hopper and Walker2D, and 200k transitions for Humanoid. The demonstration set size is roughly linear to the number of observation dimensions.

10.5 Implementation details

10.5.1 Experiment setting

We use the OpenAI gym package to construct the experiment environments and set the frame skip in all environments to 1. We use Adam optimizer and mean squared error as our loss function. During

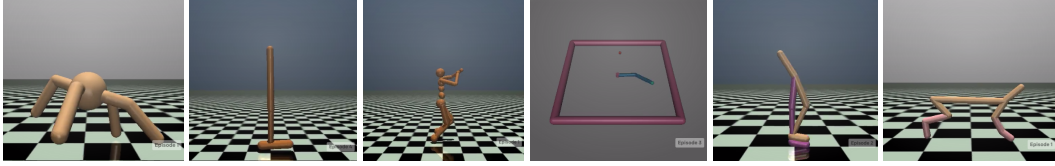


Figure 10: Snapshots of the six MuJoCo environments used in our experiments, including Ant, Hopper, Humanoid, Reacher, Walker2d and HalfCheetah (from left to right).

training, we set the number of training iterations to 300,000 and minibatch size to 64. And we decay the learning rate by 0.1 three times during the course of training.

We evaluate each model in environments at five checkpoints (280k, 285k, 290k, 295k and 300k iteration) and calculate their average rewards as the final reward.

10.5.2 Hyper-parameters

We set the learning rate of E and F network to 2×10^{-4} , the weight of adversarial loss α to 2 and the weight of KL divergence λ to 1×10^{-3} in all the environments. The hyper-parameters that differ among different environments are shown in Table 6.

Table 6: Hyper-parameters used in each environment. The embedding noise is used in all environments except Hopper and Walker2d to stabilize training.

	D learning rate	D embedding noise std
Ant	5×10^{-4}	2.0
Hopper	4×10^{-4}	-
Humanoid	4×10^{-4}	1.5
Reacher	4×10^{-4}	2.0
Walker2d	2×10^{-4}	-
HalfCheetah	4×10^{-4}	2.0

10.6 Test Loss Comparison

As shown in Table 7, the BC-OH baseline has smaller test loss than BC-SO, indicating that there is no over-fitting in training with observation histories. Thus the performance drop from BC-SO to BC-OH, such as in Humanoid, is attributed to the copycat problem. And compared with BC-OH, our method has higher test loss while producing higher reward when evaluated in the environment, showing that we’re actually solving the copycat problem rather than only reducing overfitting to training data.

Table 7: The test loss of BC-SO, BC-OH and our method under the same settings as Table 2.

	Ant	Hopper	Humanoid	Reacher	Walker2d	HalfCheetah
BC-SO	0.1079	0.0077	0.5710	0.0008	0.0410	0.1225
BC-OH	0.0829	0.0049	0.5470	0.0007	0.0136	0.0309
Ours	0.0860	0.0087	0.5632	0.0010	0.0229	0.0321